EUROPEAN FUSION DEVELOPMENT AGREEMENT

EFDA–JET–CP(01)08-05

R.D. Gill, B. Alper, M. de Baar, T.C. Hender, M.F. Johnson,
V. Riccardo and JET EFDA Contributors

Behaviour of Disruption Generated Runaways in JET

Behaviour of Disruption Generated Runaways in JET

R.D. Gill[1], B. Alper[1], M. de Baar[2], T.C. Hender[1], M.F. Johnson[1],
V. Riccardo[1] and JET EFDA Contributors

[1]EURATOM-UKAEA Fusion Association, Culham Science Centre, Abingdon, OX14 4XB, United Kingdom.
[2]FOM/Euratom Instituut voor Plasmafysica 'Rijnhuizen', Trilateral Euregio Cluster (TEC), The Netherlands

**See Annex of J. Pamela et al., "Overview of Recent JET Results and Future Perspectives", Fusion Energy 2000 (Proc. 18th Int. Conf. Sorrento, 2000), IAEA, Vienna (2001).*

Preprint of Paper to be submitted for publication in Proceedings of the
7th IAEA TCM on Energetic Particles,
(Gothenburg, 8-11 October 2001)

ABSTRACT

Experiments have established the regions of parameter space in JET that lead to runaway generation in disruptions. Previous measurements on the structure of the runaway beam have been confirmed. The delay in runaway generation following the temperature collapse is found to be caused by the very high density generated by the disruption. It is shown that runaway in JET can be best modelled and understood by including avalanche processes.

1. INTRODUCTION

The potentially damaging consequences of large runaway currents, generated by disruptions, are a possible issue for next step devices. It is therefore important to systematically study runaway current generation and control. Recent progress on such studies in JET will be reported here. A series of experiments has established the regions of parameter space leading to runaway generation and the possible role of magnetic fluctuations has been investigated. A summary of the measured properties of the runaway beams is given and a model of the generation process has been investigated to try to establish the importance of avalanche effects in JET.

The disruptions generated relativistic beams of electrons. The beams produced weak x-ray images by excitation of plasma impurity ions that allowed the determination the beam structure and development. The measurements confirmed that the runaways were initially generated close to the torus axis. Subsequently, the movement of the current column was dominated by vertical instability and an inward movement caused by the loss of plasma ß. The runaway current column showed no sign of instability.

A model of the runaway generation and development has been investigated both with and without avalanche effects. The calculations were strongly dependent on the time development of the plasma density, and a delay was found in the runaway generation caused by too high an initial plasma density. It was difficult to reproduce the time dependence of the runaway current unless avalanche effects were included. The calculations also showed very considerable differences in the relativistic electron energy spectra.

2. STATISTICAL ANALYSIS OF DISRUPTING SHOTS

A survey of JET shots that disrupt was originally made Harris [1]. He identified the variations caused by different configurations and gave examples of discharges with very long runaway tails, also reported by Wesson [2] and Gill [3]. More recently it has been reported [4] that rather few discharges had long runaway tails, although some examples were occasionally found. Judged on the presence of a current plateau after the disruption this remains correct. The failure to develop a substantial runaway current tail is attributed to the more vertically unstable plasma columns caused by the non-symmetric divertor configuration installed in 1992/3. A recent and more detailed examination of the hard x-ray emission following disruption showed that, according to this criterion, some runaways were generated in a wide variety of shots. A survey of a large

number of discharges showed, on a scatter plot of toroidal field, $ß_ø$, versus q_{95} (Fig.1), that runaways occurred after a disruption when the values of $ß_ø$ and q_{95} exceeded thresholds of 2.2T and ~2.5 respectively, although the data was quite sparse below $q_{95} < 2.5$. The probability of runaway generation reduced as q_{95} increased and increased with Bf . It was also found that the largest integrated hard x-ray yields corresponded with low elongation, although the dependence was not strong. The results are in close agreement with similar studies at JT60-U [5].

A series of experiments has been conducted to further the understanding of runaway production and to try to develop control scenarios. A systematic plasma current scan at $ß_ø = 3$ and 3.4T showed that, in discharges disrupting after strong Ar puffing, runaway formation was a maximum at I=2MA, dropping to almost zero at higher and lower currents. The data of Fig.2 shows the maximum of the hard x-ray emission versus plasma current. This is in agreement with the general overall statistics. In further experiments no runaways were found with $ß_ø < 2.5$T. It is thought that runaway beam generation does not occur at low plasma currents as the electric field is too low; at high currents, magnetic fluctuations may prevent their formation.

This idea has some support from magnetic measurements. The magnitude of magnetic fluctuations following a disruption has been estimated from the power spectrum as a function of frequency for an inner and an outer fast Mirnov coil. Data was examined between 1 and 3ms after the disruption to avoid signal saturation. Each spectrum had a characteristic plateau between 15 and 25kHz and the amplitude was determined for this band. The data from the 3T shots (Fig.3) clearly showed that the fluctuation level was correlated with the hard x-ray signal.

3. MAIN FEATURES OF DISRUPTIONS WITH RUNAWAYS

Disruptions are multi-stage events caused by too high density, current, inductance or other disturbance. The processes leading to runaway generation are well known [2] and will be repeated here for a coherent development of what follows:

1. Mhd instabilities lead to the start of the current quench and negative voltage spike;
2. The plasma temperature is reduced to low value by an influx of impurities;
3. Control of the plasma position is lost, with inward motion due to loss of plasma pressure, and usually with vertical instability;
4. The plasma current decays initially on resistive timescale;
5. The electric field rises reflecting low T_e ;
6. High loop volts cause runaway generation and a plateau develops on the current tail;
7. Copious gamma rays and some neutrons are produced when the runaways hit the wall;
8. The properties of the post-disruption plasma are poorly known.

Many of these features can be seen in Figs. 4(a) and (b). Of particular interest are the characteristic delays between the negative voltage spike and the first observation of the hard x-rays and the subsequent delay before any neutrons are seen. These delays may be interpreted as the time for

appreciable numbers of electrons to be accelerated well above the thresholds for hard x-ray production and photo-neutron production respectively. The initial delay affects the maximum energy that can be attained by the runaways.

4. PROPERTIES OF THE RUNAWAYS

A considerable advance was made in the determination of the properties of the runaway beam when measurements were made of the images of the beam by observing the radiation hardened soft x-ray cameras [4]. The runaways formed these images as a result of K-shell vacancy production in metallic ions. Ar lines can also contribute to this emission. The recent runaway campaign. has confirmed the overall picture of the structure and development of the runaway beam. A typical example of one of these images is shown in Fig. 5. From these and other standard measurements the following properties of the runaways have been reasonably well determined.

1. The clear images of the developing beams determined the size and vertical position of the beam. These measurements agreed with vertical position also found from the magnetic signals. The in-flight runaways showed no sign of instability.
2. The measurements showed that the onset of the runaway generation was a few ms after the negative voltage spike and that the runaways developed in a toroidal tube with a minor diameter up to 1.5m, initially at the vessel centre and then gradually drifting to the walls.
3. In some cases the q values of the beam was be found from the emission profile [4]. This varied from ~3 at the edge to <1 at the centre of the current distribution.

Similar results have been obtained in other experiments [6]. The energy spectrum was measured but a value of the maximum energy attained can be made by estimating the electric field at the centre of the plasma and assuming that the electrons are in free fall. This gives maximum values of up to 80 MeV.

5. MODELLING OF RUNAWAY PRODUCTION

The simplest approach to trying to understand runaway production in JET is to use a simple 0-d model. Following the negative voltage spike there is a delay before the generation of runaways and this is attributed either to the effects of magnetic fluctuations [5] or to too high a plasma density. In recent JET experiments the density during this period has been measured showing that during a disruption the density rose to a high level before decaying exponentially. In addition, the q-profile measurement [4] showed that the current density in the runaway beam was comparable, and possibly higher, than that before the disruption. This observation seems to rule out the extremely flat current profiles postulated as a development of part of the mhd part of the disruption process [7]. Under these circumstances a good insight can be obtained of the different processes by considering a column of plasma with a 1 m^2 cross-section with a current density determined by the experiment. Initially it is assumed that the plasma resistivity is uniform across

this column. This initial resistivity is derived from the experimental L/R time. The key features of the calculations are in the next section.

5.1 THE MODEL

The runaway generation rate, assuming contributions from avalanching effects, is [8]

$$dn_R/dt = n_e\, v_e\, G + n_R/\, t_a$$

where it is assumed that there no losses of electrons and n_e , v_e are the plasma density and collision rate. The avalanche growth time is:

$$t_a = 0.385\ \ m_e\, c\ \ ln\Lambda\, (2+ Z_{eff}\,)/\, eE$$

The collision rate is:

$$v_e = e^4\, n_e\, ln\Lambda\, /\, 4\, \pi\, \varepsilon_0^{\,2}\, m_e^{\,2}\, \upsilon_e^{\,3}$$

where e, m_e and u_e are the electron charge, mass and velocity. The Dreicer generation is represented by the term containing G given by:

$$G= C(Z_{eff}\,)\, exp(\, -\, 0.25/\varepsilon - (Zeff+1)^{1/2}\, \varepsilon^{\,-1/2}\ \,)\, \varepsilon^{\,-3(Zeff+1)/16}$$

with $\varepsilon = E/E_D$ and the Dreicer field $E_D = e^3\, n_e\, \ln\Lambda\, /\, 4\pi\varepsilon_0^{\,2}\, k\, T_{e.}$ The constant C is approximately given by $C = 0.21+0.11\ Z_{eff}$

Following ref [9] the electric field at constant current density is:

$$E=E_0\, (\ 1-\, j_R/\, j_0\,)\quad with\ E_0 = \eta\, j_0$$

where E_0 is the initial electric field and j_0 and j_R are the initial and runaway currents.

5.2 COMPARISON WITH EXPERIMENT

For shot 53786 the density measurements showed that n_e rose to at least 7 times its pre-disruption value and decayed exponentially with τ =5.5 ms. Z_{eff} before the disruption was 3.2 and rose considerably with argon puffing before falling near the disruption time. The plasma current decayed with time constant $\tau = L/R = 12$ ms giving a resistance of $4.2\text{x}10^{-4}\ \Omega$ for the calculated inductance of 5 μH. Assuming a uniform temperature profile this corresponds, with considerable uncertainty, to a plasma temperature of <10eV as has been previously found for JET disruptions [2]. An average loop voltage of 720V is found using this value for the temperature. This corresponds to the central value and is not therefore directly comparable with the trace of Fig. 4. The model considers the generation of runaways in a toroidal volume with a cross-sectional area of $1m^2$, and with a current density the same as the experimental value. The initial applied loop

voltage is that just calculated. The density is taken from the measured values, Z_{eff} =3.5 is assumed, and the total current density is 0.46MA/m^2. Calculations have been done (Figures 6(a) and (b)) with and without avalanching. With avalanching it is found that the growth time of the runaways and the start of the generation process are in reasonable agreement with experiment. A runaway growth time from 10% to 90% of maximum was calculated to be 5.7ms, quite near to the experimental value of 6.8ms found from the current trace (Fig.4). In particular, a delay in the generation process is found due to too high a density at early times. Once an appreciable number of runaways have been generated the value of e starts to fall and the avalanching processes becomes dominant. The delay of 3-4ms between the observation of gamma rays and neutrons can also be understood from the time development of the electron energy spectra (Figures 7(a) and (b)). Gamma rays will be observed when there is an appreciable number of runaway electrons with an energy of about 1MeV, whereas for neutron production the (γ,n) threshold of ~10MeV has to be exceeded and the peak in the photo-neutron cross-section of ~20MeV needs to be reached. The calculation is in general agreement with this. A full calculation integrating over the electron distribution and using the known bremsstrahlung and (γ,n) cross-sections would be useful.

Without avalanching it is difficult for the model to generate the full current. Again, ε falls when a few runaways are generated, but in this case the extreme sensitivity of G to small variations in ε means that runaway generation reduces sharply and the generation rate is sharply reduced. Special tailoring of the density or other parameters could artificially increase the rate.

A marked difference between the two calculations is seen in the energy spectra of the runaway electrons. With avalanching approximately exponential spectra are seen; without avalanching the spectrum has a pronounced peak at a high energy. With present diagnostics, it is not possible on JET to distinguish experimentally between these possibilities.

6. CONCLUSIONS

The regions of parameter space in JET have been identified in which disruptions lead to the generation of runaways. They appear when q_{95} and B_ϕ exceed threshold values. The overall sequence of events in the runaway development are well understood. One can conclude that avalanching is probably the dominant process in JET as it is difficult to reproduce the experimental results if this is not included in the model.

ACKNOWLEDGEMENT.

This work has been conducted under the European Fusion Development Agreement and was partly funded by Euratom and the UK Department of Trade and Industry.

REFERENCES

[1] Harris, G.R., Comparisons of the Current Decay during Carbon-bounded and Beryllium-bounded Disruptions in JET, JET-R(90)07, (1990)
[2] Wesson, J. A., Gill, R. D., Hugon, M., Sch¸ller, F.C. et al., Nuclear Fusion 29 (1989) 641
[3] Gill, R.D., Nuclear Fusion 33 (1993) 1613
[4] Gill, R.D., Alper, B., Edwards, A.W., Ingesson, L.C., Johnson, M.F. and Ward, D.J., Nuclear Fusion 40 (2000) 163
[5] Yoshino, R., Tokuda, S. and Kawano, Y., Nuclear Fusion 39 (1999)151
[6] Jaspers, R., Nuclear Fusion 36 (1996) 367
[7] Wesson, J.A., Ward, D.J. and Rosenbluth, M.N., Nuclear Fusion 30(1990) 1011
[8] Jayakumar, R., Fleichmann, H. H. and Zweben, S. J., Phys. Lett. A172 (1993) 447
[9] Rosenbluth, M. N. and Putvinsky, S.V., Nuclear Fusion 37 (1997) 1355

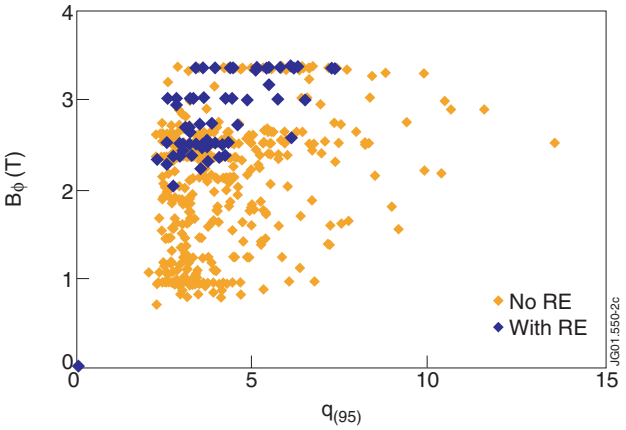

Figure 1. Scatter plot showing shots with and without runaways following disruptions as a function of β_ϕ and q_{95}. Runaways are clustered into a small part of the parameter space.

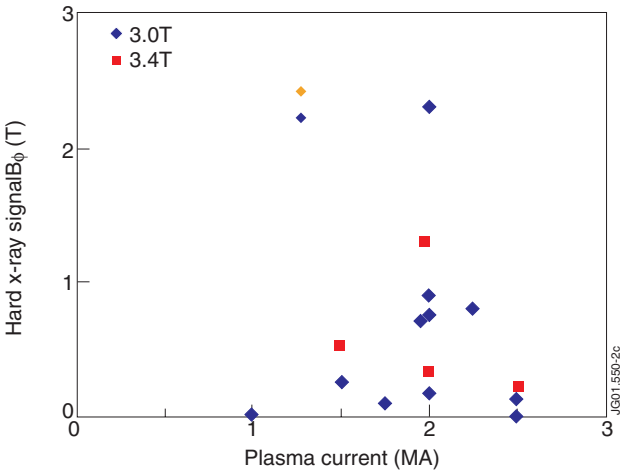

Figure 2. Dependence of the generation of hard x-rays on plasma current. The maximum of the hard x-ray signal is plotted and shows clear peaking at 2MA. The point with maximum intensity has q_{95}=3.22 and β_ϕ=3 T

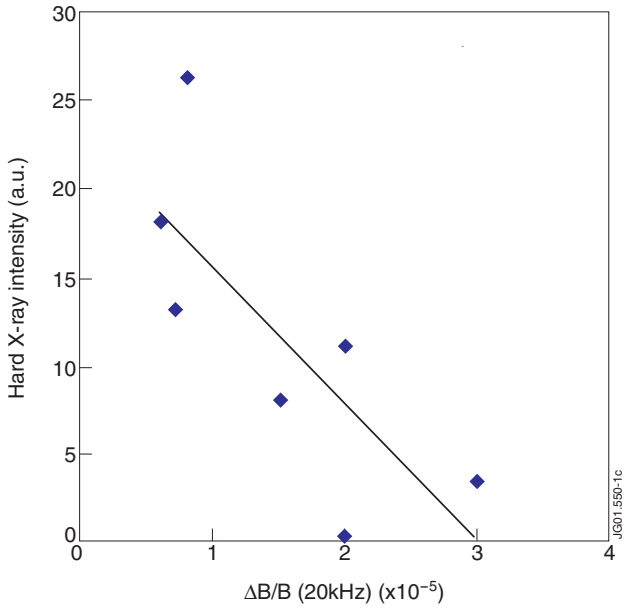

Figure 3. Variation in the hard x-ray maximum intensity with fractional poloidal magnetic field fluctuations. High levels of radiation require low fluctuation levels.

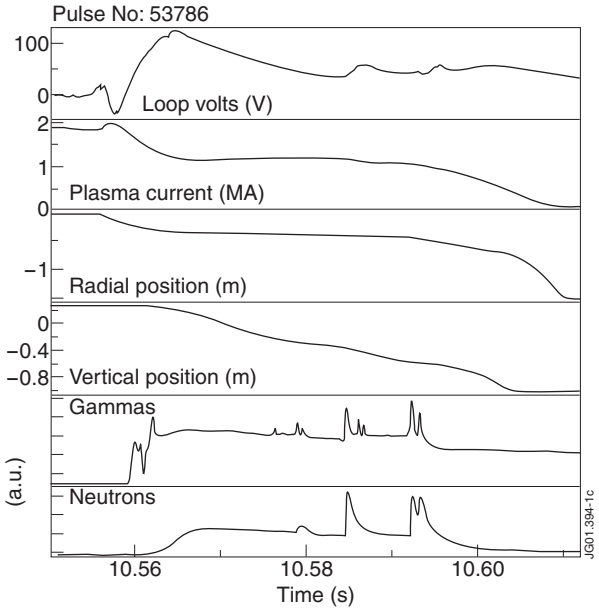

Figure.4(a): The time development in a disruption of the loop volts at the outer median plane, plasma current, position signals, gamma ray and neutron intensities

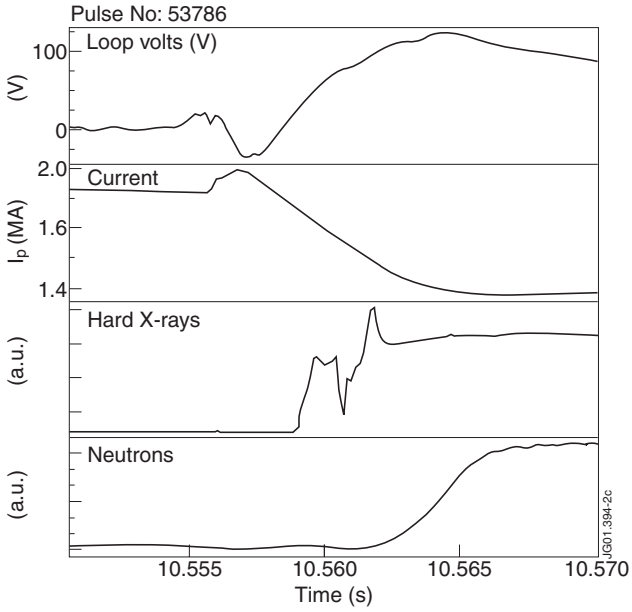

Figure.4(b): An expanded view of some of the signals of Fig 4a. The time delays between the disruption and the growth of the gamma rays and neutrons are clearly seen.

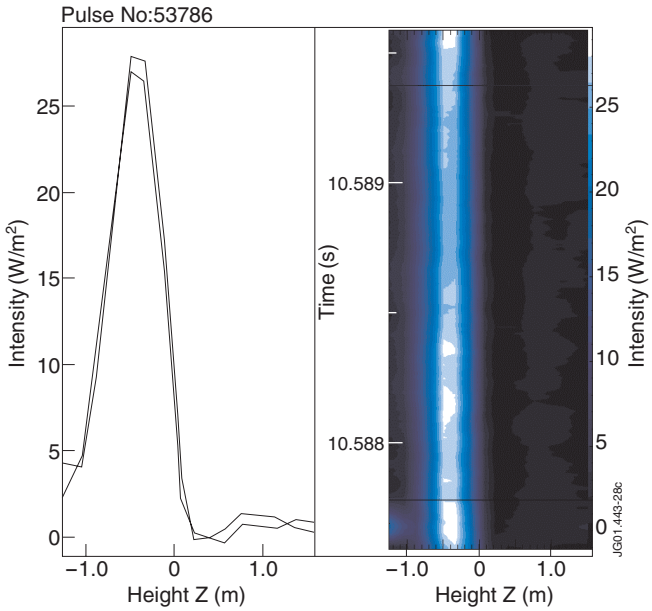

Figure 5. Soft x-ray profile and image of the runaway beam measured with a shielded soft x-ray camera.

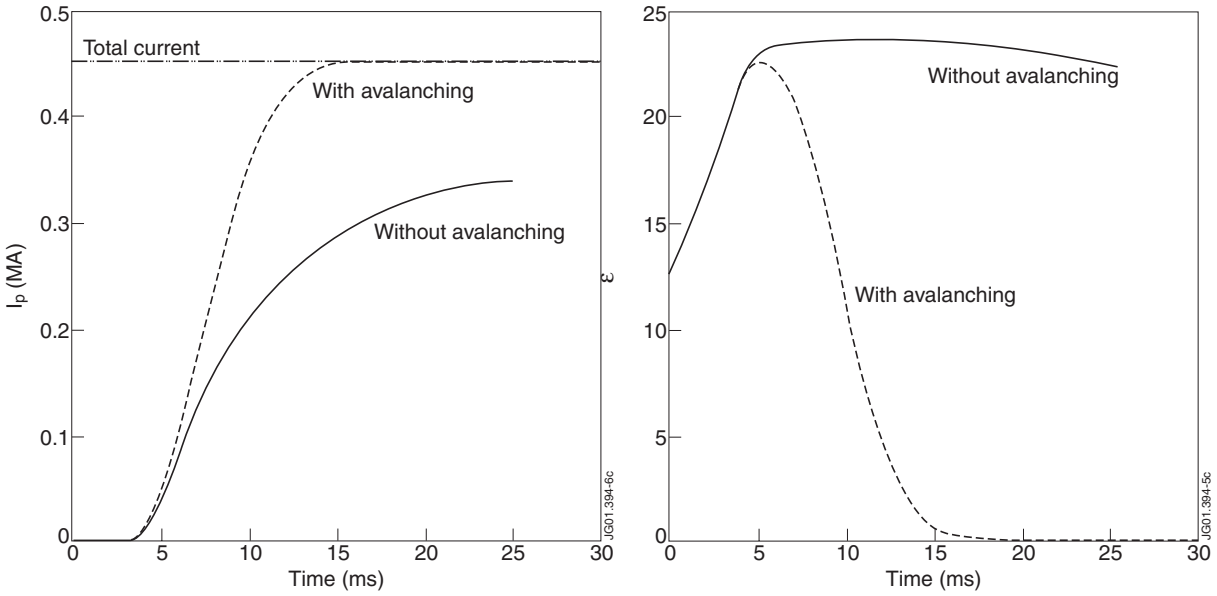

Figure.6(a) and (b): The time development of the runaway current and ε with and without avalanching.

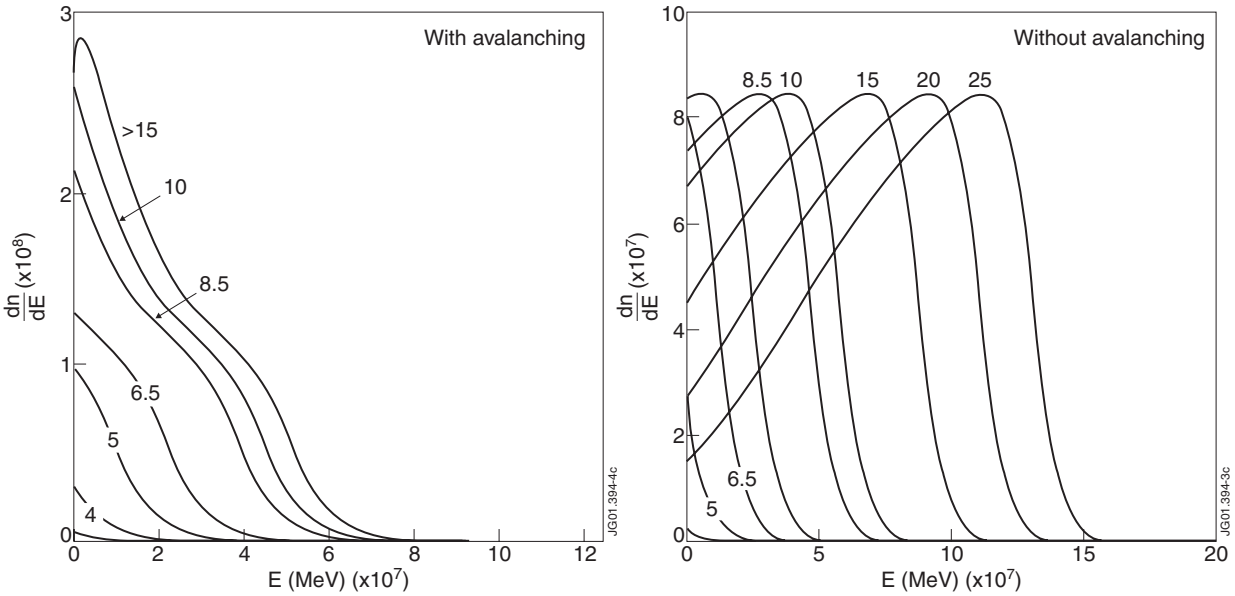

Figure.7(a) and (b): Energy spectra at different times (in ms) for calculations with and without avalanching.